Photochemical & Photobiological Sciences

Accepted Manuscript

This is an *Accepted Manuscript*, which has been through the Royal Society of Chemistry peer review process and has been accepted for publication.

Accepted Manuscripts are published online shortly after acceptance, before technical editing, formatting and proof reading. Using this free service, authors can make their results available to the community, in citable form, before we publish the edited article. We will replace this *Accepted Manuscript* with the edited and formatted *Advance Article* as soon as it is available.

You can find more information about *Accepted Manuscripts* in the Information for Authors.

Please note that technical editing may introduce minor changes to the text and/or graphics, which may alter content. The journal's standard Terms & Conditions and the Ethical guidelines still apply. In no event shall the Royal Society of Chemistry be held responsible for any errors or omissions in this *Accepted Manuscript* or any consequences arising from the use of any information it contains.

ROYAL SOCIETY OF CHEMISTRY

www.rsc.org/pps

Regulatory mechanism of ion permeation through a channelrhodopsin derived from *Mesostigma viride* (MvChR1)

Shota Watanabe[a], Toru Ishizuka[a], Shoko Hososhima[a, †], Alemeh Zamani[a], Mohammad Razuanul Hoque[a] and Hiromu Yawo[a, b, *]

Short title: Ion permeation mechanism of MvChR1

[a]Department of Developmental Biology and Neuroscience, Tohoku University Graduate School of Life Sciences and JST, CREST, Sendai 980-8577, Japan
[b]Center for Neuroscience, Tohoku University Graduate School of Medicine, Sendai 980-8575, Japan

* Correspondence to:
Hiromu Yawo Email: yawo-hiromu@m.tohoku.ac.jp
Department of Developmental Biology and Neuroscience, Tohoku University Graduate School of Life Sciences, 2-1-1 Katahira, Aoba-ku, Sendai 980-8577, Japan
Fax: + 81 22 217 6208
Tel: + 81 22 217 6211

[†]Research Fellow of Japan Society for the Promotion of Science (JSPS Research Fellow)

Abstract

The five glutamate (E) residues of transmembrane (TM)-2 of channelrhodopsin (CrChR)-2 are conserved among several members of the ChR family. A point mutation of one of them, E97 to a nonpolar alanine (E97A) reduced the photocurrent amplitude without influencing other photocurrent properties. The charge at this position is also the determinant of Gd^{3+}-dependent block of the channel. It has thus been suggested that E97 interacts with hydrated cations to facilitate their permeation and that these residues are the primary binding site of Gd^{3+}. However, the counterpart of this position is alanine for MvChR1 from *Mesostigma viride*. Here we investigated the ion permeation and the Gd^{3+}-dependent channel block of MvChR1. We found that the high-affinity binding site of Gd^{3+} was absent in MvChR1, but was dependent on the negativity at this position. However, the ion permeation through the channel was markedly interfered with a negative charge at this position. Based on these findings, it is proposed that the ions can pass through the pore with minimal interaction with this position.

Introduction

Living organisms on the earth sense light using a variety of photoreceptor molecules. For instance, in the case of a unicellular green alga, *Chlamydomonas reinhardtii*, light is sensed by two channelrhodopsins (ChRs), CrChR1 and CrChR2, which are light-sensitive cation channels.[1-4] Each ChR is a member of the microbial-type rhodopsin family and is a seven-pass transmembrane (TM) protein with a covalently bound retinal. Light absorption is followed by photoisomerization of the all-*trans* retinal to a 13-*cis* configuration and subsequent conformational changes of the molecule, which allow the channel structure to become permeable to cations.[5,6] This enables the very rapid (in the orders of ms) generation of a photocurrent in cell membranes expressing ChRs.[1,2,7,8]

It has been indicated that the five glutamate (E) residues of TM2 are involved in ion permeation.[4,9-11] Actually, a single point mutation in CrChR2 TM2 that replaced E97 with a nonpolar alanine (E97A) caused a reduction in the photocurrent amplitude without influencing other photocurrent properties, suggesting that residue E97 is involved in ion flux regulation rather than the photocycle.[10] Recently, a three-dimensional structure of a chimeric channelrhodopsin was determined in atomic resolution using a CrChR1/CrChR2 chimera termed C1C2,[12] which consists of TM1 to

TM5 from CrChR1, and TM6 and TM7 from CrChR2.[13,14] According to this, C1C2 has a water-filled outer vestibule consisting of TM1, 2, 3 and 7. The E97 (CrChR2) counterpart of C1C2 is E136, which is one of the negatively charged residues aligned along the channel pore. Similar to E97 of CrChR2, the loss of the negative charge at the position E136 position of C1C2 retarded ion permeation through the channel.[15] The charge at this position (E97 of CrChR2 or E136 of C1C2) is also a determinant of the Gd^{3+}-dependent block of the channel.[15] It has thus been suggested that both E97 (CrChR2) and E136 (C1C2) interact with hydrated cations to facilitate their permeation and that these residues are the primary binding site of Gd^{3+}.

The homologues of these ChRs have also been identified in other species together with their various properties such as the spectral sensitivity, conductance, ion selectivity, desensitization, ON and OFF kinetics.[6,16-21] These properties have been further diversified through molecular modifications.[22-25] Although the five glutamic acid residues of TM2 are conserved among many ChRs from various species, the counterparts of E83 and E97 of CrChR2 were not negatively charged in the case of MvChR1, one of ChRs derived from *Mesostigma viride*. Is the structure of the outer pore of MvChR1 different from that of C1C2 with a different manner of ion permeation? This issue was tested in the present study using an enhanced MvChR1, eMvChR1#2, in which the N-terminal segment of MvChR1 was replaced by that of CrChR2. The ion permeation and the Gd^{3+}-dependent channel block were investigated in terms of the negativity at this position of interest (the 97th residue of eMvChR1#2). We found that the high-affinity binding site of Gd^{3+} was absent in MvChR1 and eMvChR1#2, but was dependent on the negativity at this position of interest. However, as was shown previously[18], the ion permeation through the channel was markedly interfered with the negative charge at this position. It is suggested that the ion-permeating pore of MvChR1 is differently organized from that of CrChR2/C1C2 so that the ion pass through the narrowest region with minimal interaction with the counterpart position of E97/136 of CrChR2/C1C2.

Results

Improvement of MvChR1 photocurrent

Figure 1 shows the TM2 sequence of MvChR1 aligned with the corresponding sequences of other members of ChR family originating from various species (Table S1).

Although five glutamic acids of CrChR2, E82, E83, E90, E97, E101 are conserved among various algal channelrhodopsins such as CrChR1, VcChR1, VcChR2 and PsChR2, the counterparts of E83 and E97 were respectively Val and Ala in the case of MvChR1. It has been uncertain whether E83 is involved in the ion permeation.[11] On the other hand, there are accumulating evidences concerning the importance of E97 or its counterpart E136 of C1C2 as an operative constituent of the outer pore.[10-12,15] The following sections will focus on how ion permeation is regulated in MvChR1 by the charge at the counterpart position of E97(CrChR2)/E136(C1C2).

In the present study we used C1C2, which consists of TM1-5 of CrChR1 and TM6-7 of CrChR2, as a control as it is the only ChR the molecular structure of which has been investigated by crystallography.[12] When expressed in the ND7/23 cells, the photocurrent of MvChR1 was generally smaller than that of C1C2 at any wavelength of light (Fig. 2A and 2B). However, the photocurrent amplitude was significantly improved by substituting the N-terminal 56 amino acids of MvChR1 with the counterparts from CrChR1 (76 amino acids, Fig. S1, Fig. 2C) or CrChR2 (37 amino acids, Fig. S1, Fig. 2D). Our N-terminal modification likely contributes to better trafficking to the membrane as has been reported for other rhodopsins.[13,26] Both N-terminal variants, which are referred to as eMvChR1#1 and #2, exhibited similar spectral sensitivity as MvChR1 (Fig. 2E). As these channelrhodopsins showed relatively high sensitivity to the 460-490 nm-band of light, the blue LED light (460-490 nm, 0.55 $mWmm^{-2}$) was used for the following experiments in which amplitude, desensitization, turning-on time constant (τ_{ON}), shutting-off time constant (τ_{OFF}) and reversal potential (E_{rev}) were compared (Table 1). Although the photocurrent amplitude at either peak (I_{peak}) or steady state (I_{ss}) was significantly smaller for MvChR1 than for C1C2, it was significantly larger for eMvChR1#1 or #2 than for MvChR1. The magnitude of desensitization was similar among MvChR1, eMvChR1#1 and #2, but significantly less than that of C1C2. Both τ_{ON} and τ_{OFF} were similar among MvChR1, eMvChR1#1 and #2, but tended to be a little larger than those of C1C2. No significant difference was present in the E_{rev} among C1C2, MvChR1, eMvChR1#1 and #2. Therefore, except for the amplitude, the N-terminal modifications did not affect the photocurrent properties of MvChR1.

Photocurrent block by Gd^{3+}

A number of ion channels have been identified by their specific blocking agents, such as natural toxins, synthetic chemicals, metal ions, etc.[27] Most, if not all, of the blocking

agents reduced the ion flux through the channel by interacting with a molecular constituent of the channel within the pore region. The CrChR2 photocurrent was potently and reversibly blocked by Gd^{3+}, which is one of the selective blockers of stretch-activated channels, through interaction with E97 at TM2, and the C1C2 photocurrent was blocked by Gd^{3+} at its counterpart E136.[15] Indeed, Gd^{3+} potently blocked the C1C2 photocurrent at 0.3 mM (range, 61-89% of peak and 72-96% of plateau, n = 15) (Fig. 3A and 3E). On the other hand, the blocking by Gd^{3+} was significantly small for MvChR1 (range, 20-59% of peak and 25-67% of plateau, n = 12) (Fig. 3B and 3F). A similar magnitude of blocking was observed for eMvChR1#1 and #2 (Fig. 3C, 3D, 3G, and 3H).

The *I-V* relationship of the photocurrent was not linear and was rectified inwardly for C1C2, MvChR1, eMvChR1#1 and #2 (Fig. 3E-H). Although Gd^{3+} (0.3 mM) significantly retarded g_{in} for MvChR1 (50 ± 3%; $P < 0.001$, Wilcoxon signed rank test; n = 12), eMvChR1#1 (46 ± 3%; $P < 0.005$, Wilcoxon signed rank test; n = 7) and eMvChR1#2 (38 ± 3%; $P < 0.0001$, Wilcoxon signed rank test; n = 19), the magnitude was significantly smaller than that of C1C2 (86 ± 3%; $P < 0.0001$, Wilcoxon signed rank test; n = 19) (Fig. 4A and 4B). In the presence of 0.3 mM Gd^{3+}, the *I-V* relationship was outwardly rectified for C1C2 with an *RI* of 1.5 ± 0.1 (n = 15), but not for MvChR1 (0.49 ± 0.05, n = 12), eMvChR1#1 (0.58 ± 0.03, n = 6) and eMvChR1#2 (0.61 ± 0.03, n = 19) (Fig. 4C).

In summary the above effects of Gd^{3+} did not vary among MvChR1, eMvChR1#1 and #2, but were less remarkable than those on C1C2. For the following analysis we focused on eMvChR1#2 with its relatively high S/N ratio. Figures 5A shows the dose-responsiveness of steady-state g_{in} to Gd^{3+}. Each K_D value was predicted from the one-to-one binding model of Michaelis-Menten kinetics and was respectively 23 ± 10 μM (C1C2, n = 9) and 260 ± 70 μM (eMvChR1#2, n = 13) with significant difference ($P < 0.005$, Mann-Whitney *U*-test) (Fig. S2). Although I_{peak} evaluated a transient state, its apparent K_D values were 47 ± 15 μM (C1C2, n = 11) and 320 ± 100 μM (eMvChR1#2, n = 13) (Fig. 5B) with significant difference ($P < 0.005$, Mann-Whitney *U*-test) (Fig. S2). For both g_{in} and I_{peak}, relatively large Gd^{3+}-resistant components remained for eMvChR1#2. Therefore, the high-affinity site of Gd^{3+} was absent in eMvChR1#2.

Effects of A97-targeted mutation

It has been suggested that both E97 (ChR2) and E136 (C1C2) are the primary binding

sites of Gd^{3+}.[15] Although the corresponding site was conserved as Glu in the ChRs of various species, it was Ala in the case of MvChR1. To test the possible involvement of this site in the Gd^{3+} sensitivity, we investigated the eMvChR1#2 mutants of A97E, A97D, A97Q and A97R. Both the A97E and A97D mutation significantly reduced the photocurrent amplitude and conductance, whereas A97Q rather improved them (Fig. 6A-C and Table 2). The photocurrent of the A97R mutant was almost negligible. The *I-V* relationship was significantly less rectified in the A97E and A97D mutants than in eMvChR1#2 or its A97Q mutant (Fig. 6D-F and Table 2). These mutations did not significantly affect the E_{rev}, but the difference between A97E and A97D was significant.

As shown in Fig. 6A and 6B, the photocurrents of A97E and A97D were markedly blocked by 0.3 mM Gd^{3+}. Indeed, these mutations shifted the dose-response relationship toward a reduced Gd^{3+} concentration with significantly small apparent K_D values (A97E, 33 ± 12 μM, n = 11 and A97D, 37 ± 8 μM, n = 10 vs. eMvChR1#2, 260 ± 70 μM) and small Gd^{3+}-resistant components (Fig. 7 and S2). In contrast, the A97Q mutation insignificantly affected the dose-response relationship (apparent K_D, 160 ± 30 μM, n = 12).

Discussion

Based on the crystallographic three-dimensional structure of one of the chimeric channelrhodopsins, C1C2, which consists of TM1 to TM5 from CrChR1, and TM6 and TM7 from CrChR2, TM2 forms the extracellular pore of a channel with TM1, TM3 and TM7.[12] It has been assumed that E129 (TM2), E136 (TM2), E140 (TM3), E162 (TM3) and D292 (TM7) are aligned along the pore. Indeed the cationic flux was shown to be retarded by the removal or reversal of the negative charge at each position.[10,12,28] These negative charges are conserved in many known ChRs; e.g., they are respectively, E90, E97, E101, E123 and D253 in the case of CrChR2. However, the reduction of photocurrent by the neutralization of D253 (D292 of C1C2) position may be attributed to the retardation of conformational changes that gate the channel to be open since the negativity at this position make it a primary Schiff base proton acceptor.[12,29] On the other hand, the counterparts were respectively E107, A114, E118, E140 and D270 in the case of MvChR1.[18] Although four of five negative charges are conserved, the counterpart of E136 is a neutral alanine. Indeed the E136 (C1C2) and the E97 (CrChR2) were critical to the cation permeation of these ChRs and the conductance was markedly retarded by substitution with neutral alanine or glutamine or positive lysine or

arginine.[10,15,28] Furthermore, the negative charge at this site was also necessary for the channel to be blocked by Gd^{3+}. In this study we focused on the Gd^{3+} sensitivity of MvChR1.

However, the photocurrent of MvChR1 was relatively small when expressed in the conventional culture cells such as HEK293 cells and ND7/23 cells. We thus replaced the N-terminal extracellular segment of MvChR1 with the counterpart from CrChR1 (1-76) or CrChR2 (1-37) and produced eMvChR1#1 and #2. As a result, the photocurrent amplitude was enhanced by about 10 fold without affecting other properties such as desensitization, τ_{ON} and τ_{OFF}. The *I-V* relationship was also similar among MvChR1, eMvChR1#1 and #2 in terms of the *RI* and E_{rev}. The photocurrents of eMvChR1#1 and #2 were blocked by Gd^{3+} to a similar extent as that of MvChR1. The Gd^{3+} effects were also similar among these molecules in terms of the *I-V* relationship. Therefore, the modification of the N-terminal segment appears to have negligible influence on the fundamental properties of MvChR1 such as the spectral sensitivity, the photocycle kinetics, the ionic selectivity and the sensitivity to a blocker. Taken together, the above similarities supported our use of eMvChR1#2 as a substitute for native MvChR1 for investigating the mechanism of ion permeation.

Previously, it was reported that Gd^{3+} reversibly blocked both the CrChR2 and C1C2 photocurrents with K_D values as low as 7.8 μM (CrChR2) and 14 μM (C1C2).[15] Although Gd^{3+} (0.3 mM) strongly attenuated both the peak and plateau of the C1C2 photocurrent, its effects were relatively small on the photocurrent of MvChR1 or its enhanced variants in the present experiments. Indeed the K_D value of eMvChR1#2 was predicted to be 260 ± 70 μM (n = 13) from the dose-responsiveness of steady-state g_{in} to Gd^{3+}, which was one magnitude larger than that of C1C2 (23 ± 10 μM, n = 9). Moreover, there remained a significant fraction of Gd^{3+}-resistant components for both the g_{in} and I_{peak} of eMvChR1#2. It is thus suggested that the high-affinity Gd^{3+} binding site was absent in eMvChR1#2 and the Gd^{3+} binding to its low-affinity site blocked the cation flux in an incomplete manner. When blocked by Gd^{3+}, the *I-V* curve of the C1C2 photocurrent was less rectified, or even outwardly rectified. The increase of the *RI* suggests that the cationic influx was more selectively blocked than the efflux and that the high-affinity Gd^{3+} binding sites lie in the outer pore region of the channels. On the other hand the effects of Gd^{3+} on the *RI* of eMvChR1#2 were negligible, being consistent with the notion that the low-affinity site is minimally involved in the cation influx.

The lack of a high-affinity binding site for Gd^{3+} could be attributed to the loss of negativity at the 97th residue of eMvChR1#2, which is the counterpart of E97 of

CrChR2 or E136 of C1C2. Indeed the photocurrents of the A97E or A97D mutants of eMvChR1#2 were more sensitized to Gd^{3+}, with significantly small apparent K_D values to a similar extent as that of C1C2 (Fig. S2). On the other hand, the mutation to a non-negative residue such as A97Q insignificantly changed the Gd^{3+} sensitivity. It is thus suggested that A97 of eMvChR1#2 is one of the amino acid residues constituting the outer pore structure of the cationic channel, being similar to E97 of CrChR2 or E136 of C1C2.[11,12] The negativity at this position thus determines the interaction between the blocker and the channel.

In a water-filled channel, the interaction between a permeating cation and the water is the major determinant of the mobility of the ion.[27] It has been hypothesized that E97 of CrChR2 or its counterpart, E136 of C1C2, facilitates the ion permeation through its interactions with the permeating cations.[15] Consistent with this notion, the loss of negativity at this position strongly reduced the cationic influx through the channel.[10,15,28] In contrast, the addition of negativity at the corresponding position of eMvChR1#2 markedly attenuated the photocurrent, with a significant increase in the *RI*. Therefore, the inward permeation of cations was at least interfered with the Ala-to-Glu or –Asp exchange at this position. The contradictory effects of negatively charged residues between CrChR2/C1C2 and MvChR1 could be attributed to a difference in the structure of the narrowest pores. For example, the size of the narrowest pores may be relatively small in the case of CrChR2 or C1C2. Based on the relative permeability of permeating ions, the minimum pore diameter of 6.22 Å has been calculated for CrChR2,[30] the value smaller than that of the nicotinic acetylcholine receptor (6.5-7 Å) but larger than that of the voltage-dependent Na^+ channel (3-5 Å).[2] Therefore, the permeating cation has to be partially dehydrated before passing through the selective filter. In the case of eMvChR1#2, the permeating cations should be dehydrated interacting with negatively charged amino-acid residues around the pore, such as E101 (TM2), E123 (TM3) and D253 (TM7).[12] For the A97E or A97D mutants, the additional interaction between the permeating ion and the carboxyl group should retard the speed of ion transport. For the A97R mutant the additional positive charge in the outer vestibule may hinder the access of cations to the narrowest pore region through electric repulsion. Such a structural difference could also influence the ion selectivity of the channel. Indeed, the *I-V* relationship of eMvChR1#2 was more dependent on the concentration gradient of Na^+ or K^+ than that of C1C2 (Fig. S3). Similarly, the ratio of Na^+ to H^+ permeability in MvChR1 is much higher than the ratio in CrChR2[19] whereas CrChR2 was more permeable to H^+.[2] As the H^+ permeability is almost independent of the pore size,[27] the larger flow rate of Na^+ should be the critical mechanism underlying the higher Na^+

permeability of the MvChR1 channel. However, the precise mechanisms of ion permeation have to be experimentally studied further using crystallography and site-directed mutagenesis in combination. The eMvChR1#1 and #2 would contribute these future studies.

Experimental

Plasmids

Plasmids encoding CrChR1, CrChR2, and MvChR1 were gifts from T. Takahashi (Toho University, Funabashi, Japan), G. Nagel (University of Würzburg, Germany), and J. L. Spudich (University of Texas Medical School, Houston, TX, USA), respectively. DNA fragments encoding MvChR1(M1-R323), eMvChR1#1, an N-terminal variant of MvChR1 that consists of M1-L76 from CrChR1 and H57-R323 from MvChR1, and eMvChR1#2, another N-terminal variant that consists of M1-A37 from CrChR2 and H57-R323 from MvChR1, were produced by conventional PCR or overlap extension PCR using KOD -Plus- DNA polymerase (TOYOBO, Osaka, Japan) and subcloned in-frame into pVenus-N1 as described previously.[13] C1C2, a chimeric molecule that consists of the TM1-5 of CrChR1 and the TM6-7 of CrChR2, subcloned in-frame into pVenus-N1 has been described previously.[13] Point mutations were introduced using a KOD-Plus- Mutagenesis Kit (TOYOBO). All constructs were verified by sequencing.

Cell culture

The electrophysiological assays of ChRs and their variants were made using ND7/23 cells, a hybrid cell line derived from neonatal rat dorsal root ganglia neurons fused with the mouse neuroblastoma.[31] ND7/23 cells were grown in Dulbecco's modified Eagle's medium (Wako, Osaka, Japan) supplemented with 2.5 μM all-*trans* retinal, 10% fetal bovine serum under a 5% CO_2 atmosphere at 37 °C. The expression plasmids were transiently transfected in ND7/23 cells using Effectene Transfection Reagent (Qiagen, Tokyo, Japan) according to the manufacturer's instructions. Electrophysiological recordings were then conducted 16-48 h after the transfection. Successfully transfected cells were identified by the presence of Venus fluorescence.

Electrophysiology

All experiments were carried out at room temperature (23 ± 2 °C). Photocurrents were recorded as previously described[8] using an EPC-8 amplifier (HEKA Electronic,

Lambrecht, Germany) under a whole-cell patch clamp configuration. The data were filtered at 1 kHz and sampled at 10 kHz (Digidata1440 A/D, Molecular Devices Co., Sunnyvale, CA) and stored in a computer (pClamp10.3, Molecular Devices). The absence of dye coupling was confirmed by visualization of Alexa 568 (Life Technologies, Carlsbad, California, USA).

The internal pipette solutions for the whole-cell voltage-clamp recordings from ND7/23 cells contained (in mM) 120 KOH, 100 glutamate, 5 EGTA, 50 HEPES, 2.5 $MgCl_2$, 2.5 MgATP, 0.1 Leupeptin, 0.1 QX-314, 0.01 Alexa 568, adjusted to pH 7.3 with KOH. The extracellular ACSF solution contained (in mM) 125 NaCl, 2.5 KCl, 25 $NaHCO_3$, 1.25 NaH_2PO_4, 2 $CaCl_2$, 1 $MgCl_2$, 11 glucose, bubbled with mixed gas containing 95% O_2 and 5% CO_2. To investigate the Gd^{3+} effects, we used a Tyrode's solution consisting of (in mM) 138 NaCl, 4 NaOH, 3 KCl, 10 HEPES, 2 $CaCl_2$, 1 $MgCl_2$, 11 glucose, bubbled with O_2 gas. The liquid junctional potential was directly measured as -6.7 mV and was compensated.

The photocurrent amplitude and kinetics are dependent on the irradiance,[8] the holding potential[1,2,8] and the pH.[1,2,32] Therefore, every photocurrent was measured with a holding potential of -66.7 mV and at pH 7.4 outside. For the spectral sensitivity, each photocurrent evoked by 1-s irradiation was measured and the amplitude was averaged between on- and offset of the light pulse. Otherwise, the photocurrents were evoked by 3-s irradiation of blue LED light.

The current-voltage (*I-V*) relationship was obtained by applying a 1-s voltage ramp (from -66.7 to 53.3 mV) during the steady-state of the photocurrent with subtraction of the leak *I-V* curve obtained before irradiation. The photocurrent peak amplitude was expressed as an effective value (I_{peak}) after being divided by the whole-cell capacitance, which is proportional to the cell's surface area. For evaluating the magnitude of desensitization, the difference between the peak photocurrent and the steady-state photocurrent (I_{ss}) at the end of a 3-s light pulse was divided by I_{peak}. The slope between -66.7 mV and the reversal potential was divided by the whole-cell capacitance and expressed as an effective inward conductance (g_{in}). Similarly, the effective outward conductance (g_{out}) was calculated from the slope between +53.3 mV and the reversal potential. The rectification index (*RI*) was defined as $RI = g_{out}/g_{in}$.

Each photocurrent ON kinetics was fitted by a single-exponential function of the time during the transition phase between 10 and 90% of the I_{peak} without any obvious deviation from the raw data. In the case of OFF kinetics, the photocurrent transient after 3-s irradiation was fitted by a single-exponential function of the time between 90 and 10% of the I_{ss}.

Optics

To investigate the action spectrum, irradiation was carried out using a SpectraX light engine (Lumencor Inc., Beaverton, OR) controlled by computer software (pCLAMP10.3, Molecular Devices) at wavelengths (nm, > 90% of the maximum): 390 ± 18, 438 ± 24, 475 ± 28, 513 ± 17, 549 ± 15, 575 ± 25 and 632 ± 22. The power of light was directly measured under microscopy by a visible light-sensing thermopile (MIR-100Q, Mitsubishi Oil Chemicals, Tokyo, Japan) and was adjusted to 0.5 $mWmm^{-2}$ on the specimen.

To investigate the Gd^{3+} effects, we used a power LED (Philips Lumileds Lighting Inc., San Jose, CA) emitting blue light (peak, 460-490 nm, LXHL-NB98) controlled by a regulator (SLA-1000-2, Mightex, Toronto, Canada) and computer software (pCLAMP10.3, Molecular Devices). The power of light on the specimen was 0.55 $mWmm^{-2}$. The interval between pulses was set to 20 s to ensure the full recovery of photocurrent (Fig. S4).[18]

Statistical analysis

All data in the text, figures and tables are expressed as mean ± SEM and were evaluated with the Kruskal-Wallis test for statistical significance unless otherwise noted. It was judged as statistically insignificant when $P > 0.05$.

Conclusion

This paper provides additional evidences that the structure of ion-permeating pore varies among ChRs, a family of light-sensitive ion channels of microbial rhodopsins. Although the negativity of the E97 position of CrChR2 facilitated the cation permeation, it is not always conserved in some ChRs such as those from *Asteromonas gracilis*-B (AgChR),[21] *Proteomonas sulcata* (PsChR1),[21] *Chloromonas subdivisa* (CsChR),[21] and *Dunaliella salina* (DsChR1).[33] It remains to be investigated what else structures are involved in the cation permeation through pore. As MvChR1 is more selective to Na^+ than ChR2,[19] further modification of the molecule could enable its optimization for optogenetic applications.

Acknowledgements

We thank Drs. J. L. Spudich and E. G. Govorunova (University of Texas Medical School, Houston, Texas 77030, U. S. A.) for comments on the manuscript as well as for MvChR1 cDNA, and B. Bell for language assistance. This work was supported by Grant-in-Aid for Japan Society for the Promotion of Science (JSPS) Fellows (Number, 13J06372), scientific research from the Ministry of Education, Culture, Sports, Science and Technology (MEXT) of Japan (Numbers, 25290002, 25670103, 25250001, 25115701), Global COE Program (Basic & Translational Research Center for Global Brain Science), MEXT and the Program for Promotion of Fundamental Studies in Health Sciences of the National Institute of Biomedical Innovation (NIBIO).

References

1. G. Nagel, D. Ollig, M. Fuhrmann, S. Kateriya, A. M. Musti, E. Bamberg and P. Hegemann, Channelrhodopsin-1: a light-gated proton channel in green algae, *Science*, 2002, **296**, 2395-2398.
2. G. Nagel, T. Szellas, W. Huhn, S. Kateriya, N. Adeishvili, P. Berthold, D. Ollig, P. Hegemann and E. Bamberg, Channelrhodopsin-2, a directly light-gated cation-selective membrane channel, *Proc Natl Acad Sci U S A*, 2003, **100**, 13940-13945.
3. O. A. Sineshchekov, K. H. Jung and J. L. Spudich, Two rhodopsins mediate phototaxis to low- and high-intensity light in *Chlamydomonas reinhardtii*, *Proc Natl Acad Sci U S A*, 2002, **99**, 8689-8694.
4. T. Suzuki, K. Yamasaki, S. Fujita, K. Oda, M. Iseki, K. Yoshida, M. Watanabe, H. Daiyasu, H. Toh, E. Asamizu, S. Tabata, K. Miura, H. Fukuzawa, S. Nakamura and T. Takahashi, Archaeal-type rhodopsins in *Chlamydomonas*: model structure and intracellular localization, *Biochem Biophys Res Commun*, 2003, **301**, 711-717.
5. C. Bamann, T. Kirsch, G. Nagel and E. Bamberg, Spectral characteristics of the photocycle of channelrhodopsin-2 and its implication for channel function, *J Mol Biol*, 2008, **375**, 686-694.
6. O. P. Ernst, P. A. Sanchez Murcia, P. Daldrop, S. P. Tsunoda, S. Kateriya and P. Hegemann, Photoactivation of channelrhodopsin, *J Biol Chem*, 2008, **283**, 1637-1643.
7. E. S. Boyden, F. Zhang, E. Bamberg, G. Nagel and K. Deisseroth, Millisecond-timescale, genetically targeted optical control of neural activity, *Nat*

Neurosci, 2005, **8**, 1263-1268.

8. T. Ishizuka, M. Kakuda, R. Araki and H. Yawo, Kinetic evaluation of photosensitivity in genetically engineered neurons expressing green algae light-gated channels, *Neurosci Res*, 2006, **54**, 85-94.
9. P. Hegemann, Algal sensory photoreceptors *Annu Rev Plant Biol*, 2008, **59**, 167-189.
10. Y. Sugiyama, H. Wang, T. Hikima, M. Sato, J. Kuroda, T. Takahashi, T., Ishizuka and H. Yawo, Photocurrent attenuation by a single polar-to-nonpolar point mutation of channelrhodopsin-2, *Photochem Photobiol Sci*, 2009, **8**, 328-336.
11. H. C. Watanabe, K. Welke, F. Schneider, S. Tsunoda, F. Zhang, K. Deisseroth, P. Hegemann and M. Elstner, Structural model of channelrhodopsin, *J Biol Chem*, 2012, **28**, 7456–7466.
12. H. E. Kato, F. Zhang, O. Yizhar, C. Ramakrishnan, T. Nishizawa, K. Hirata, J. Ito, Y. Aita, T. Tsukazaki, S. Hayashi, P. Hegemann, A. D. Maturana, R. Ishitani, K. Deisseroth and O. Nureki, Crystal structure of the channelrhodopsin light-gated cation channel, *Nature*, 2012, **482**, 369-374.
13. H. Wang, Y. Sugiyama, T. Hikima, E. Sugano, H. Tomita, T. Takahashi, T. Ishizuka and H. Yawo, Molecular determinants differentiating photocurrent properties of two channelrhodopsins from *Chlamydomonas*, *J Biol Chem*, 2009, **284**, 5685-5696.
14. S. P. Tsunoda and P. Hegeman, Glu 87 of channelrhodopsin-1 causes pH-dependent color tuning and fast photocurrent inactivation, *Photochem Photobiol*, 2009, **85**, 564–569.
15. S. Tanimoto, Y. Sugiyama, T. Takahashi, T. Ishizuka and H. Yawo, Involvement of glutamate 97 in ion influx through photo-activated channelrhodopsin-2. *Neurosci Res*, 2013, **75**, 13-22.
16. F. Zhang, M. Prigge, F. Beyriere, S. P. Tsunoda, J. Mattis, O. Yizhar, P. Hegemann and K. Deisseroth, Red-shifted optogenetic excitation: a tool for fast neural control derived from *Volvox carteri*, *Nat Neurosci*, 2008, **11**, 631-633.
17. A. Kianianmomeni, K. Stehfest, G. Nematollahi, P. Hegemann and A. Hallmann, Channelrhodopsins of *Volvox carteri* are photochromic proteins that are specifically expressed in somatic cells under control of light, temperature, and the sex inducer. *Plant Physiol*, 2009, **151**, 347-366.
18. E. G. Govorunova, E. N. Spudich, C. E, Lane, O. A. Sineshchekov and J. L. Spudich, New channelrhodopsin with a red-shifted spectrum and rapid kinetics from *Mesostigma viride*, *mBio*, 2011, **2**, e00115-11.

19. E. G. Govorunova, O. A. Sineshchekov, H. Li, R. Janz and J. L. Spudich, Characterization of a highly efficient blue-shifted channelrhodopsin from the marine alga *Platymonas subcordiformi*, *J Biol Chem*, 2013, **288**, 29911-29922.
20. S. Y. Hou, E. G. Govorunova, M. Ntefidou, C. E. Lane, E. N. Spudich, O. A. Sineshcheko and J. L. Spudich, Diversity of *Chlamydomonas* channelrhodopsins, *Photochem Photobiol*, 2012, **88**, 119-128.
21. N. C. Klapoetke, Y. Murata, S. S. Kim, S. R. Pulver, A. Birdsey-Benson, Y. K. Cho, T. K. Morimoto, A. S. Chuong, E. J. Carpenter, Z. Tian, J. Wang, Y. Xie, Z. Yan, Y. Zhang, B. Y. Chow, B. Surek, M. Melkonian, V. Jayaraman, M. Constantine-Paton, G. K. Wong and E. S. Boyden, Independent optical excitation of distinct neural populations, *Nat Methods*, 2014, **11**, 338–346.
22. J. Mattis, K. M. Tye, E. A. Ferenczi, C. Ramakrishnan, D. J. O'Shea, R. Prakash, L. A. Gunaydin, M. Hyun, L. E. Fenno, V. Gradinaru, O. Yizhar and K. Deisseroth, Principles for applying optogenetic tools derived from direct comparative analysis of microbial opsins, *Nat. Methods*, 2012, **9**, 159-172.
23. J. Y. Lin, P. M. Knutsen, A. Muller, D. Kleinfeld and R. Y. Tsien, ReaChR: a red-shifted variant of channelrhodopsin enables deep transcranial optogenetic excitation, *Nat Neurosci*, 2013, **16**, 1499-1508.
24. J. Wietek, J. S. Wiegert, N. Adeishvili, F. Schneider, H. Watanabe, S. P. Tsunoda, A. Vogt, M. Elstner, T. G. Oertner and P. Hegemann, Conversion of channelrhodopsin into a light-gated chloride channel, *Science*, 2014, **344**, 409-412.
25. A. Berndt, S. Y. Lee, C. Ramakrishnan and K. Deisseroth, Structure-guided transformation of channelrhodopsin into a light-activated chloride channel, *Science*, 2014, **344**, 420-424.
26. V. Gradinaru, K. R. Thompson and,K. Deisseroth, eNpHR: a *Natronomonas* halorhodopsin enhanced for optogenetic applications, *Brain Cell Biol*, 2008, **36**, 129-139.
27. B. Hille, *Ion channels of excitable membranes, third ed.*, Sinauer Associates, Massachusetts, USA, 2001.
28. K. Ruffert, B. Himmel, D. Lall, C. Bamann, E. Bamberg, H. Betz and V. Eulenburg, Glutamate residue 90 in the predicted transmembrane domain 2 is crucial for cation flux through channelrhodopsin 2, *Biochem Biophys Res Commun*, 2011, **410**, 737-743.
29. V. A. Lórenz-Fonfría and J. Heberle, Channelrhodopsin unchained: structure and mechanism of a light-gated cation channel. *Biochim Biophys Acta*, 2014 **1837**, 626-642.

30. R. Richards and R. E. Dempski, Re-introduction of transmembrane serine residues reduce the minimum pore diameter of channelrhodopsin-2, *PLoS One*, 2012, **7**, e50018.
31. J. N. Wood, S. J. Bevan, P. R. Coote, P. M. Dunn, A. Harmar, P. Hogan, D. S. Latchman, C. Morrison, G. Rougon, M. Theveniau and S. Wheatley, Novel cell lines display properties of nociceptive sensory neurons, *Proc Biol Sci*, 1990, **241**, 187–194.
32. P. Hegemann, S. Ehlenbeck and D. Gradmann, Multiple photocycles of channelrhodopsin, *Biophys J*, 2005, **89**, 3911–3918.
33. F. Zhang, J. Vieroch, O. Yizhar, L. E. Fenno, S. Tsunoda, A. Kianianmomeni, M. Prigge, A. Berndt, J. Cushman, J. Polle, J. Magnuson, P. Hegemann and K. Deisseroth, The microbial opsin family of optogenetic tools, *Cell*, 2011 **147,** 1446-1457.
34. F. Sievers, A. Wilm, D. G. Dineen, T. J. Gibson, K. Karplus, W. Li, R. Lopez, H. McWilliam, M. Remmert, J. Söding, J. D. Thompson and D. Higgins, Fast, scalable generation of high-quality protein multiple sequence alignments using Clustal Omega, *Mol Syst Biol*, 2011 **7,** 539.

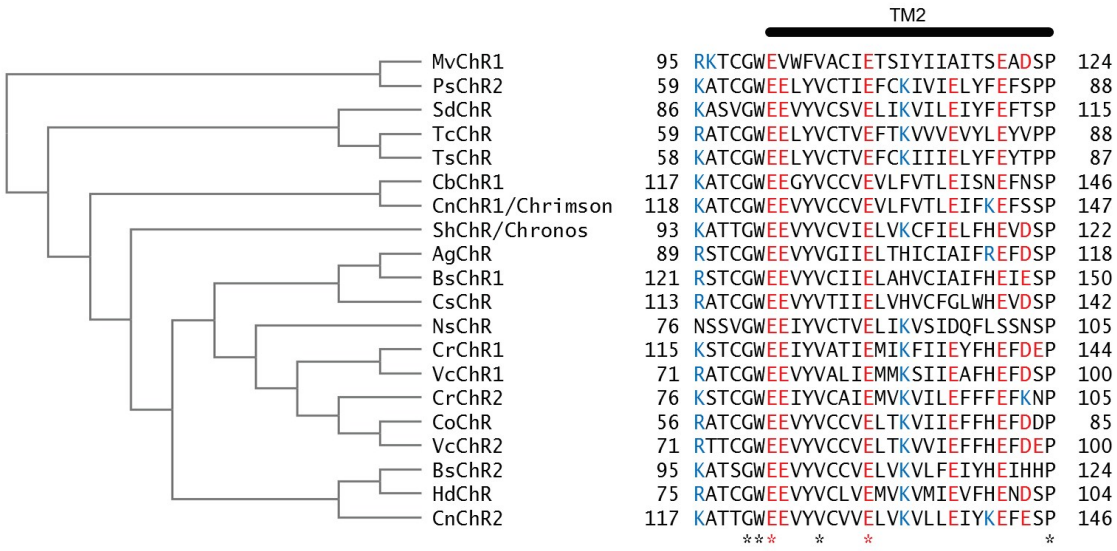

Fig. 1 Comparison of known algal channelrhodopsins. *Left*, phylogenic tree showing homology among molecules.[34] *Right*, amino acid sequence alignment of the second transmembrane domain (TM2). Acidic residues are indicated in red and basic residues are in blue. *, the identical amino acids among all species indicated above (Table S1). TM2 is indicated by a black line according to the crystal structure of C1C2.

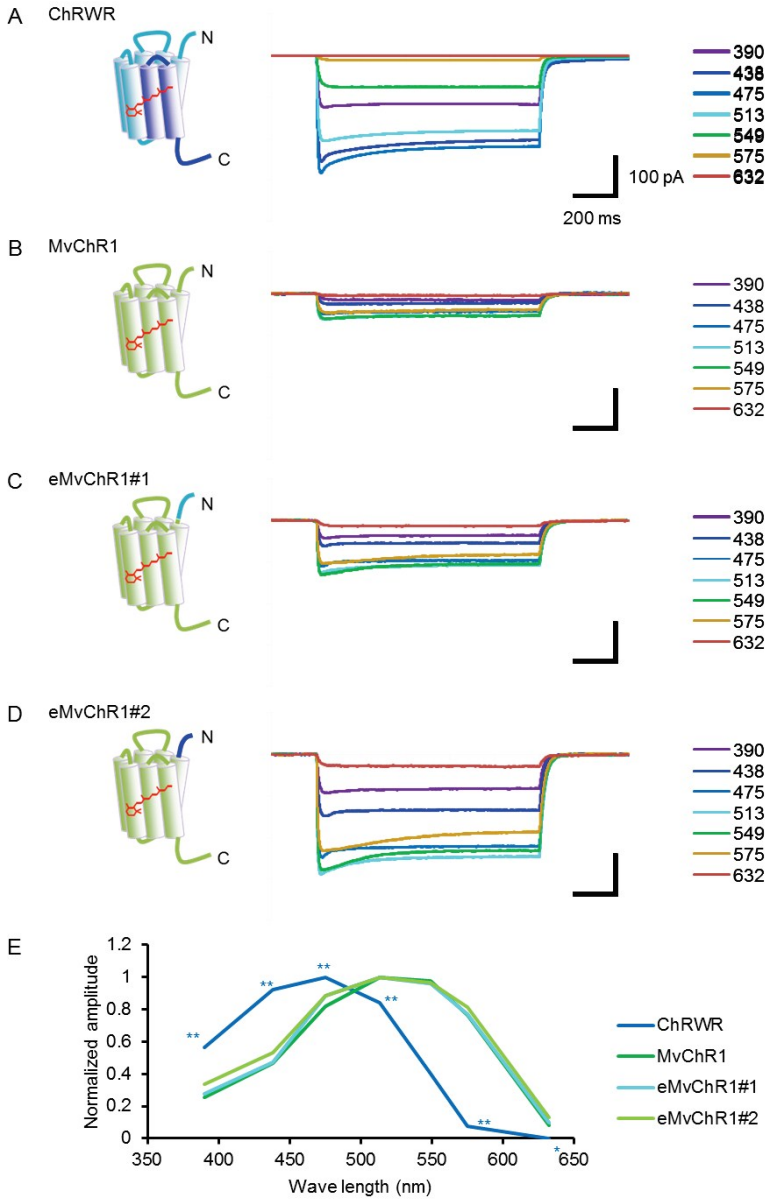

Fig. 2 Improvement of MvChR1 photocurrent. (A)-(D) Sample photocurrents of C1C2 (A), MvChR1 (B), eMvChR1#1 (C) and #2 (D) to each wavelength of light (nm, > 90% of the maximum): 390 ± 18, 438 ± 24, 475 ± 28, 513 ± 17, 549 ± 15, 575 ± 25 and 632 ± 22. The power of each was adjusted to 0.5 $mWmm^{-2}$. Scale bars, 200 ms and 100 pA for all records. (E) Comparison of the spectral sensitivity. Each average amplitude normalized to the maximal value of each photocurrent; C1C2 (n = 6), MvChR1 (n = 7), eMvChR1#1 (n = 8) and #2 (n = 7). *, $P < 0.05$ and **, $P < 0.01$, one-way ANOVA with Scheffé post hoc test against MvChR1.

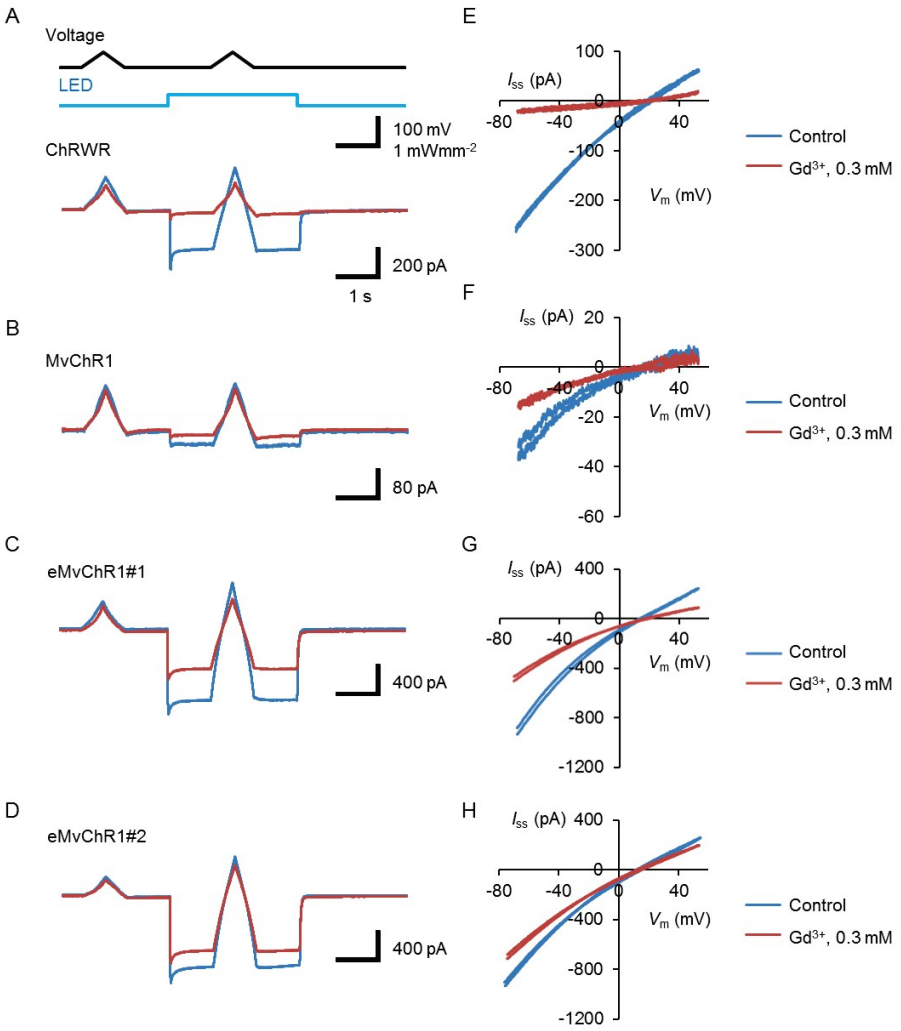

Fig. 3 Photocurrent block by Gd^{3+}. (A)-(D) Sample photocurrents of C1C2 (A), MvChR1 (B), eMvChR1#1 (C) and #2 (D) with (red) and without (blue) 0.3 mM Gd^{3+}. The holding potential for each was -66.7 mV. Scale bars, 1 s and 200 pA for (A), 80 pA for (B) while 400 pA for (C) and (D). The top and middle traces in (A) are respectively changes of voltage and irradiation, which are also applied to (B)-(D). Scale bars, 1 s and 100 mV or 1 $mWmm^{-2}$. (E)-(H) Current-voltage (*I-V*) relationships obtained from the corresponding sample photocurrent records with (red) and without (blue) 0.3 mM Gd^{3+}.

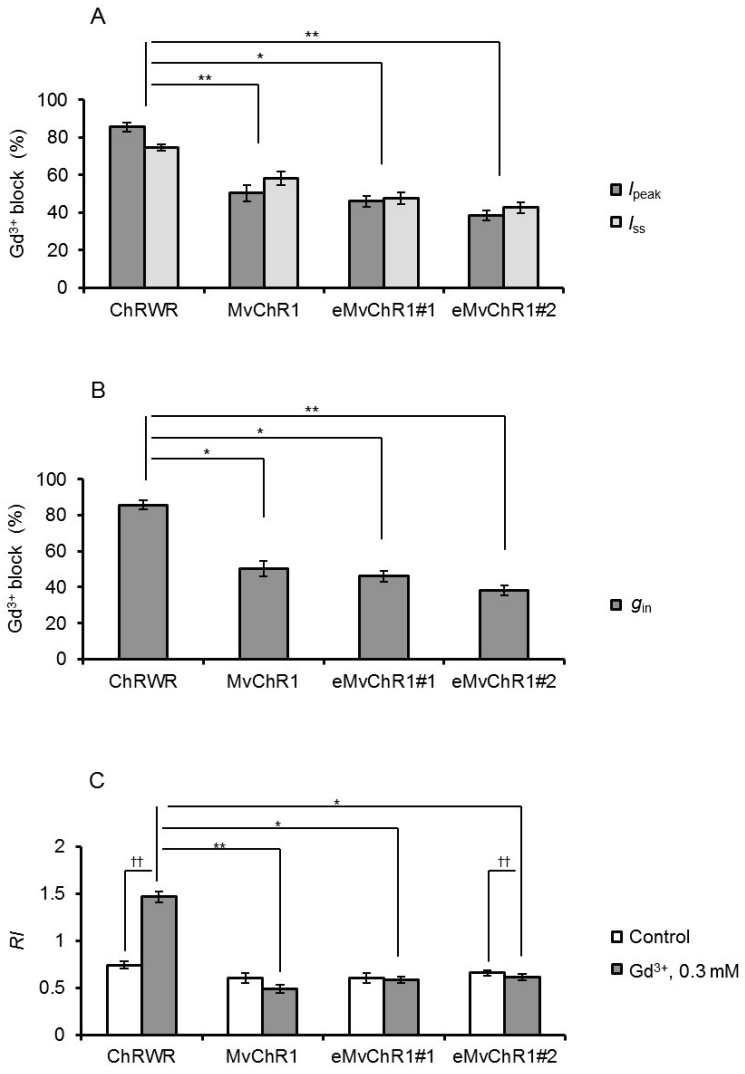

Fig. 4 Summary of Gd^{3+} effects. (A) Effects of 0.3 mM Gd^{3+} on the peak (I_{peak}) and steady-state photocurrents (I_{ss}). (B) Effects of 0.3 mM Gd^{3+} on the effective inward conductance (g_{in}). (C) Rectification indices in the absence (open columns) and the presence (closed columns) of 0.3 mM Gd^{3+}. *, $P < 0.05$ and **, $P < 0.01$ (Kruskal-Wallis test) and ††,$P < 0.01$ (Wilcoxon signed-rank test).

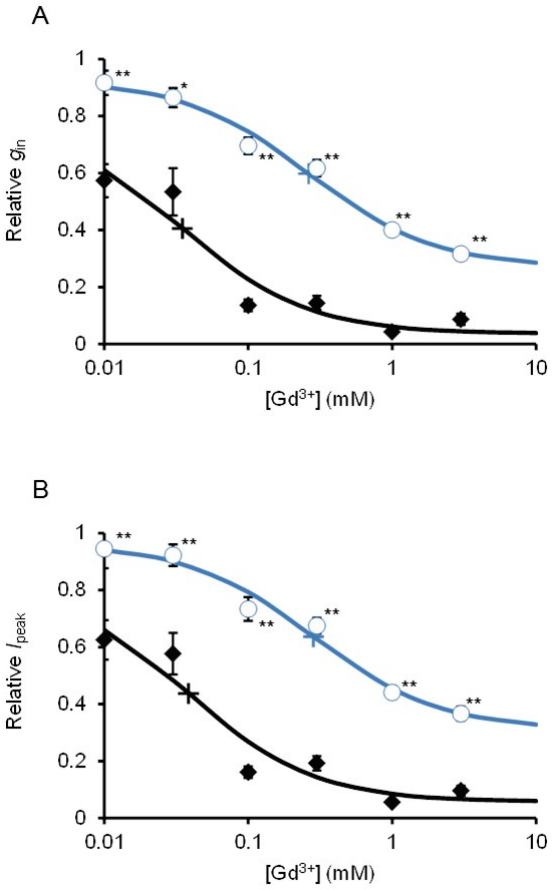

Fig. 5 Gd^{3+} sensitivity. (A) Dose-response relationship of g_{in} to Gd^{3+}; C1C2 (closed diamonds, n = 6~17) and eMvChR1#2 (open circles, n = 6~18). Each line is the least squares fitting to the Michaelis-Menten relationship with constant $y = a\{1–x/(x+b)\}+c$; black line for C1C2 (a = 0.74, b = 0.035 mM and c = 0.036), blue line for eMvChR1#2 (a = 0.66, b = 0.26 mM and c = 0.27). (B) Dose-response relationship of I_{peak} to Gd^{3+}; C1C2 (closed diamonds, n = 6~17) and eMvChR1#2 (open circles, n = 6~21). Each line is the least squares fitting to the Michaelis-Menten relationship with constant $y = a\{1–x/(x+b)\}+c$; black line for C1C2 (a = 0.76, b = 0.038 mM and c = 0.057), blue line for eMvChR1#2 (a = 0.65, b = 0.28 mM and c = 0.31). *, P<0.05; **, P<0.005; Mann-Whitney *U*-test.

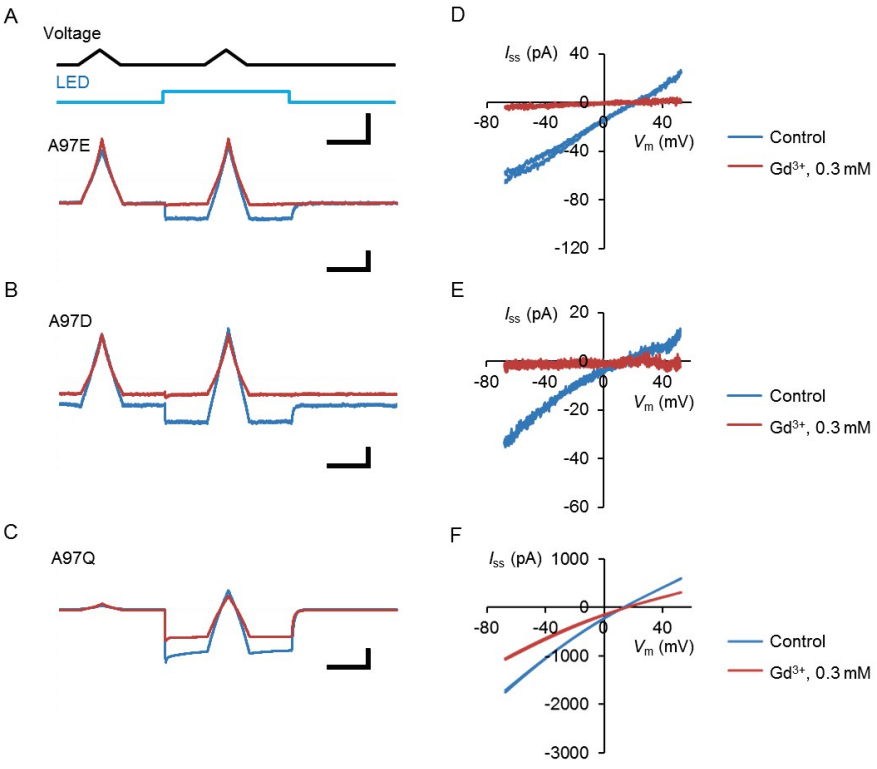

Fig. 6 Effects of A97-targeted mutation. (A)-(C) Sample photocurrents of A97E (A), A97D (B) and A97Q (C) mutants of eMvChR1#2 with (red) and without (blue) 0.3 mM Gd^{3+}. The holding potential was each -66.7 mV. Scale bars, 1 s and 80 pA for (A), 40 pA for (B) and 800 pA for (C). The top and middle traces in (A) are respectively changes of voltage and irradiation, which are also applied to (B) and (C). Scale bars, 1 s and 100 mV or 1 $mWmm^{-2}$. (D)-(F) Current-voltage (*I-V*) relationships obtained from the corresponding sample photocurrent records with (red) and without (blue) 0.3 mM Gd^{3+}.

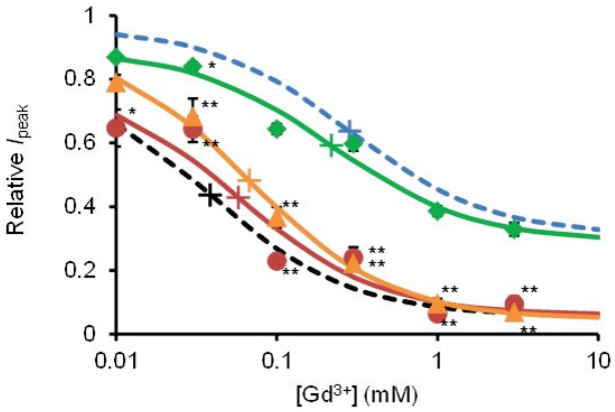

Fig. 7 Gd^{3+} sensitivities of A97-targeted mutants. Dose-response relationship of I_{peak} to Gd^{3+}; A97E (red circles, n = 5~14) A97D (orange triangles, n = 4~6) and A97Q (green diamonds, n = 6). Each line is the least squares fitting to the Michaelis-Menten relationship with constant $y = a\ \{1–x/(x+b)\}+c$; red line for A97E (a = 0.73, b = 0.058 mM and c = 0.060), orange line for A97D (a = 0.87, b = 0.067 mM and c = 0.047) and green line for A97Q (a = 0.60, b = 0.22 mM and c = 0.29). Broken lines are respectively C1C2 (black) and eMvChR1#2 (blue) for reference. Statistical significance was tested against eMvChR1#2 with Mann-Whitney U-test and indicated as *, P<0.05; **, P<0.005.

Table 1 Photocurrent properties of C1C2, MvChR1, eMvChR1#1 and eMvChR1#2 expressed in ND7/23 cells.

	C1C2 (36)	MvChR1 (13)	eMvChR1#1 (7)	eMvChR1#2 (35)
I_{peak} (pA)	610 ± 60	62 ± 10**	880 ± 230††	970 ± 230††
I_{ss} (pA)	400 ± 40	53 ± 9**	730 ± 190††	770 ± 170††
Desensitization	0.36 ± 0.02	0.18 ± 0.04**	0.19 ± 0.01**	0.18 ± 0.01**
τ_{ON} (ms)	1.9 ± 0.1	2.3 ± 0.1*	2.4 ± 0.3	2.2 ± 0.1*
τ_{OFF} (ms)	17 ± 1	18 ± 1	20 ± 1	20 ± 1**
E_{rev} (mV)	12 ± 3	20 ± 2	20 ± 2	18 ± 2

*, $P < 0.05$ and **, $P < 0.01$ from C1C2 (Kruskal-Wallis test)
†, $P < 0.05$ and ††, $P < 0.01$ from MvChR1 (Kruskal-Wallis test)

Table 2 Summary of the effects of negativity at A97 position of eMvChR1#2

	eMvChR1#2 (35)	A97E (25)	A97D (13)	A97Q (12)	A97R (5)
I_{peak} (pA)	970 ± 230	64 ± 10**††	37 ± 3**††	1400 ± 300	4.4 ± 1.4**††
I_{ss} (pA)	770 ± 170	45 ± 0**††	19 ± 3**††	1300 ± 300	3.5 ± 1.5**††
g_{in} (nS/pF)	0.32 ± 0.06	0.028 ± 0.005**††	0.016 ± 0.002**††	0.66 ± 0.15	
g_{out} (nS/pF)	0.23 ± 0.05	0.029 ± 0.005**††	0.014 ± 0.001**††	0.35 ± 0.08	
RI	0.67 ± 0.02	1.0 ± 0.1**††	0.88 ± 0.06††	0.51 ± 0.02	
E_{rev} (mV)	18 ± 2	26 ± 2	16 ± 3‡	22 ± 3	

*, $P < 0.05$ and **, $P < 0.01$ from eMvChR1#2 (Kruskal-Wallis test)

†, $P < 0.05$ and ††, $P < 0.01$ from A97Q (Kruskal-Wallis test)

‡, $P < 0.05$ from A97E (Kruskal-Wallis test)

Graphical abstract

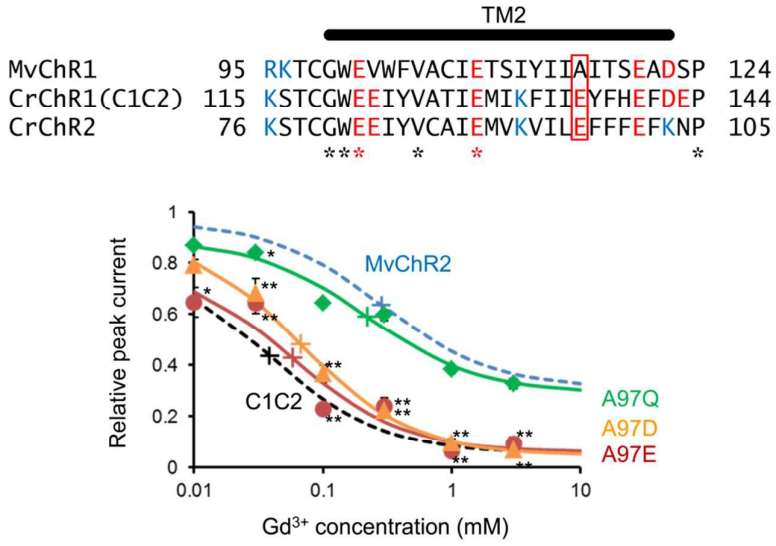

MvChR2 was rather insensitive to Gd^{3+} because of the absence of negativity at the 116th position, which is glutamate in the case of channelrhodopsin-2 (CrChR2) or the C1C2.